Available online at www.sciencedirect.com
ScienceDirect
Geomorphology 82 (2006) 84–97
GEOMORPHOLOGY
www.elsevier.com/locate/geomorph

Debris dams and the relief of headwater streams

Stephen T. Lancaster [a,*], Gordon E. Grant [b]

[a] Department of Geosciences, Oregon State University, 104 Wilkinson Hall, Corvallis, OR 97331-5506, USA
[b] PNW Research Laboratory, USDA Forest Service, Corvallis, OR 97331, USA

Received 15 September 2004; received in revised form 30 August 2005; accepted 30 August 2005
Available online 12 June 2006

Abstract

In forested, mountain landscapes where debris flows are common, their deposition commonly forms valley-spanning dams of wood, boulders, or complex mixtures of both in headwater valleys. Sediment impoundment behind these dams causes alluviation in what would otherwise be bedrock channels. In this paper, the effects of debris dams on the evolution of headwater valley profiles over geologic time are examined. In the Oregon Coast Range, USA, longitudinal profiles of three headwater channels (approximately 2 km^2 maximum contributing area), two of which are nominally bedrock, and all debris dams were surveyed. Channel and valley widths were measured, and surface bed material measurements (pebble counts) were taken at several locations along one stream. Cumulative relief in debris dams is highly variable within and among streams, reaching a maximum of 58% of profile relief at one location. The surveyed dams comprise 9.8%, 19%, and 6.4% of total basin relief in the three corresponding drainage basins, respectively. A model of bedrock erosion and channel profile evolution is derived that accounts for (a) fractional coverage by the channel of total valley width at any given time and (b) shielding by sediment impounded behind debris dams. The equation for incision rate, assumed constant, is solved for valley gradient as a function of contributing area, and parameter values are estimated from or supplied by field data. Results are compared to stream-gradient–contributing-area relationships obtained for the field sites. These comparisons suggest a strong effect of network structure, which varies significantly among the sites, on profile shape and relief because of the different susceptibilities to debris-flow deposition and, therefore, debris-dam formation. Longitudinal profiles with and without the effects of debris dams are modeled for one forced-alluvial, i.e., nominally bedrock, channel. For these model profiles, which extend only as far as the surveyed profile at this site, 55% of the profile relief is due to debris dams and the concomitant shielding of the bed by impounded sediment. The results suggest that a significant fraction of the relief of such forested, mountain landscapes is due to the effects of relatively immobile wood and boulders deposited in the valleys by debris flows.

Keywords: Debris; Drainage patterns; Landform evolution; Natural dams; Relief; Stream gradient

1. Introduction

In forested headwater streams and valleys at the transition between mass-movement and fluvial processes, sediment delivery from the hillslopes to the valley and channel network is apparently dominated by mass-movement processes (Eaton et al., 2003), but sediment

* Corresponding author. Tel.: +1 541 737 9258; fax: +1 541 737 1200.
E-mail address: Stephen.Lancaster@geo.oregonstate.edu (S.T. Lancaster).

0169-555X/$ - see front matter © 2006 Elsevier B.V. All rights reserved.
doi:10.1016/j.geomorph.2005.08.020

export is dominated by fluvial processes. Far from "chutes" that quickly transport all sediment supplied from upstream, the transport capacity of streams is episodically overwhelmed by volumes of wood, boulders, gravel, and finer sediment that may be stored for centuries or longer (Casebeer, 2004). This debris-flow–fluvial transition is a major linkage between geomorphic processes in headwater stream-valley systems and is therefore important for understanding the sediment budget of larger stream systems, including those delivering sediment to salmonid-spawning habitat and sinks on the continental shelf.

Several aspects of the debris-flow–fluvial transition distinguish it from other parts of the hillslope–fluvial system. First, sediments are stored on the valley bottom in landforms that morphologically appear to be floodplains and are genetically similar to floodplains in some ways, but the processes building these sediment bodies are largely debris-flow deposition or backwater deposition by fluvial processes upstream of debris dams. Second, these valleys have underlying bedrock strath surfaces apparently formed by lateral migration, but that migration is driven by avulsions due to debris-flow and wood deposition. Third, many valleys are aggraded and are typically five times wider than their respective channels, but are generally part of an actively incising network. Finally, wood and boulders cause avulsions, control grade, and store sediment in these valleys in a manner qualitatively similar to that which occurs within lower gradient streams, but quantities are typically far greater at the debris-flow–fluvial transition.

Debris-flow deposition in the Oregon Coast Range typically forms valley-spanning debris dams that are composed primarily of wood and impound significant sediment volumes, although some dams result from riparian treefall. These impoundments typically fill with sediment to form steps and force nominally bedrock channels to be alluvial (Montgomery et al., 1996; Massong and Montgomery, 2000; Montgomery et al., 2003b; Fig. 2). Wood thus affects the amounts and patterns of sediment storage in drainage networks (Swanson and Lienkaemper, 1978; Marston, 1982; Nakamura and Swanson, 1993; Lancaster et al., 2001; May and Gresswell, 2003) and also affects smaller features such as the locations and morphologies of pools (Buffington et al., 2002). Montgomery et al. (2003a) surmised that the relative immobility of large wood, its impounding of sediment, and the concomitant shielding of the underlying bedrock decrease the effective bedrock erodibility and, hence, steepen the longitudinal channel profile. These effects are likely greater further upstream because (a) debris flows richer in wood deposit further upstream (May, 2002; Lancaster et al., 2003) and (b) large wood has lower mobility in smaller channels (Marcus et al., 2002). Boulders, which are deposited by debris flows but which are essentially immovable by fluvial processes, have similar effects (Fig. 2).

This paper examines the effects of debris dams of wood and boulders on longitudinal profile relief and gradient at the debris-flow–fluvial transition at three sites in the Oregon Coast Range, USA (Fig. 1), although the results are largely generalizable to other mountain streams in which debris dams form. Here a conceptual model is presented that attributes gradient and relief of mountain streams to three components: (a) the debris dams, (b) gradients of channels in alluvium impounded behind those dams, and (c) resistance of the underlying bedrock to erosion. For the third component, the "stream-power law" of bedrock incision provides a framework for evaluating the effects of the other two because these streams, with notable exceptions, are bedrock controlled. The main hypothesis of this paper is that debris dams and their associated sediment impoundments have an important effect on that control by shielding the bedrock from the erosive tools of the streams (e.g., Sklar and Dietrich, 1998, 2001). A simple model based on the stream-power law and utilizing data from the Oregon Coast Range illustrates this effect.

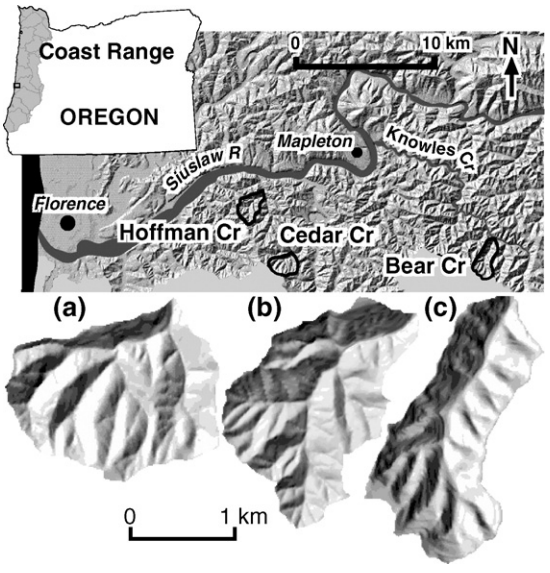

Fig. 1. Top: map of the Oregon Coast Range with locations of Cedar Creek, Hoffman Creek, and Bear Creek sites (outlined with solid lines). Bottom: enlarged shaded-relief maps of the (a) Cedar Creek, (b) Hoffman Creek, and (c) Bear Creek sites. See Table 1 for elevation ranges.

2. Field sites in the Oregon Coast Range, USA

Field work was conducted in three drainage basins in the Oregon Coast Range: (a) a tributary to Cedar Creek ("Cedar Creek"), (b) a tributary to Hoffman Creek ("Hoffman Creek"), and (c) Bear Creek (Fig. 1, Table 1). These basins were chosen for their similar lithologies and drainage areas, but different shapes, and the fact that neither valley-bottom nor mid-slope roads have affected debris-flow runout and deposition in the mainstem valleys (Swanson et al., 1977). The basins are underlain by massive, gently dipping, rhythmic interbedded sandstone and siltstone of the Eocene Tyee Formation except for the southern-most part of the Cedar Creek basin, which is underlain by intrusive volcanic rocks of an unnamed formation (Peck, 1961), which may have thermally altered and thus hardened nearby sandstone. Topography in the basins is steep–valley sideslopes are typically ca. 40°–and highly dissected. Soils are shallow and have low bulk densities (e.g., Reneau and Dietrich, 1991, measured values of ~1 kg/m^3 at a similar site in the Oregon Coast Range). The climate is maritime with warm, dry summers and mild, wet winters. Diffusive hillslope transport processes and debris flows deliver sediment to the valley network (e.g., Dietrich and Dunne, 1978; Benda, 1990).

In this part of the Oregon Coast Range, forest biomass is typically less than but of the same order of magnitude as the mass of the soil layer, especially in mature stands (Grier and Logan, 1977; Sidle, 1992; Duan, 1996; Heimsath et al., 2001). The forest is primarily Douglas fir (*Pseudotsuga menziesii*) and secondarily western hemlock (*Tsuga heterophylla*), western red cedar (*Thuja plicata*), red alder (*Alnus rubra*), and bigleaf maple (*Acer macrophyllum*). Douglas fir, western hemlock, and western red cedar typically reach breast-height diameters (DBH) in excess of 2 m in "old-growth" (i.e., older than ~250 years) stands. Wood is therefore a significant part of the mass moved by landslides and debris flows and an important structural element in the beds of stream channels, where it can remain for decades or longer (Hyatt and Naiman, 2001). After wood decays within debris dams, a boulder lag originally trapped by the wood often remains, and this stoney accumulation may persist indefinitely (Fig. 2). Parts of all of the sites have been harvested in the last half-century, but at some sites, many large, cut logs were left in low-order channels and are found in many debris dams.

3. Field and analytical methods

The main channels of the study basins were surveyed with hand level and tape measure during the summer of 2000. Steps in the profile were surveyed in detail, and notes were taken regarding their characteristics, whether in the bedrock itself or made of debris dams composed of wood, boulders, or a mixture of the two (i.e., wood-and-boulder jam). Dam height was defined as the difference between the minimum of elevations upstream of the dam and the maximum of elevations downstream of the dam, i.e., plunge-pool depths and wood and boulder heights above channel beds were excluded. Profile surveys continued upstream, as feasible, to include all significant valley-floor deposits. Stream gradients were calculated from the profiles between 10-m vertical intervals, as in Snyder et al. (2000). The ratio of dam height to spacing was calculated as the average height of two adjacent dams divided by the horizontal distance between them.

Surveyed longitudinal channel profiles were matched to those extracted from digital elevation models (DEMs) by transforming the extracted profiles to match known locations of tributary junctions and basin outlets. Contributing areas at every surveyed point were interpolated from DEM-derived values associated with points along the transformed, extracted profiles. Stream gradients were associated with contributing areas at the upstream ends of the intervals for gradient calculation. Dam height-to-spacing ratios were associated with

Table 1
Drainage basin characteristics for the study sites

Site	Description	Drainage area (km^2)	Elevation range (m)	Circularity [a]	β, θ, R^2 from slope-area fits [b]
Cedar Creek	Right-bank tributary of Cedar Creek, 1.8 km upstream of Sweet Creek confluence	1.84	79–539	0.796	43.5, 0.445, 0.685
Hoffman Creek	Left-bank tributary of Hoffman Creek, 1.7 km upstream of Siuslaw River confluence	2.03	10–265	0.596	208, 0.631, 0.965
Bear Creek	Left-bank tributary of Knowles Creek	2.19	97–480	0.514	283, 0.612, 0.828

[a] Circularity is defined as $(4\pi A)/P^2$, where A is drainage basin area and P is drainage basin perimeter (Mayer, 1990).
[b] $S=\beta A^{-\theta}$, where S is stream gradient; A is contributing area in m^2; β is the steepness coefficient with units, $m^{2\theta}$; and θ is the concavity index.

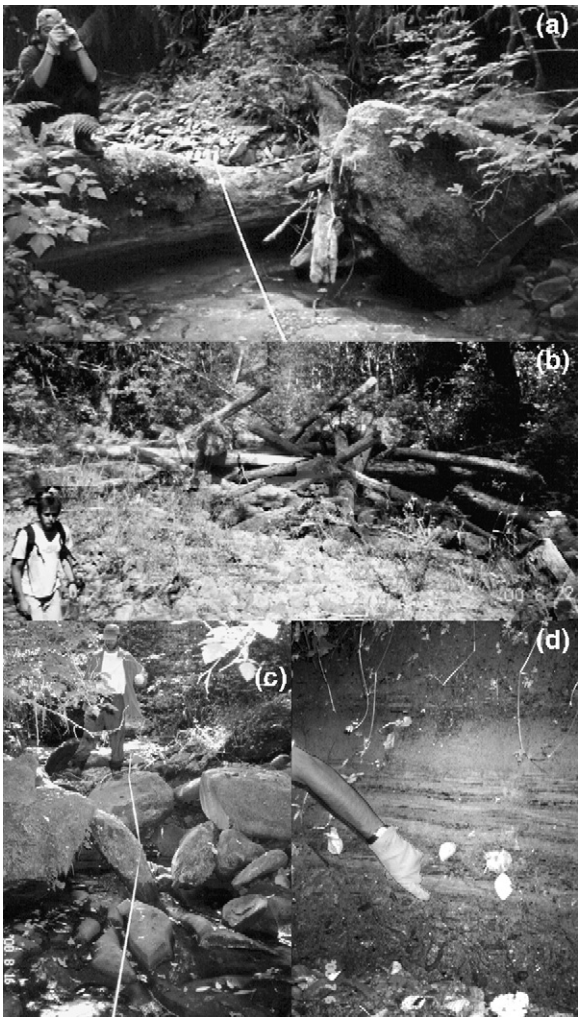

Fig. 2. (a) View upstream of single-log dam in Bear Creek. (b) View downstream of sediment wedge impounded behind debris dam formed by wood-and-boulder jam in Bear Creek site, ~1700 m upstream of outlet. (c) View upstream of boulder jam in Bear Creek site, 1150 m upstream of outlet. (d) Debris-dam–impounded, incised deposit of fine-sediment and organic-material strata onlapping a debris-flow deposit, i.e., massive and poorly sorted with matrix-supported, angular clasts, 640 m upstream of the outlet of the Hoffman Creek site. Finger is pointing to debris-flow–fluvial contact, which dips to the right, or upstream (downstream is to the left). The debris flow apparently issued from a right-bank tributary with a nearly 90° confluence angle with the main channel, dammed it, and formed slack water in which fine sediments and organic material were deposited.

contributing areas at the downstream dam because the spacing is meant to be the distance downstream from the last dam. (Also, for sites where power-law fits between dam height-to-spacing ratio and contributing area explained significant amounts of the ratio's variance, those amounts were higher, i.e., greater R^2, when using contributing area at downstream dams.)

Measurements and observations of the channel and valley were also made. At intervals of approximately 10 channel widths, valley and incised-channel widths were measured, and scale photographs of the bed were taken. Valley width is the horizontal distance between steep (40–60°) valley walls. At tributary mouths, the valley edge is the imaginary line connecting the upstream and downstream valley walls. Incised-channel width is the distance between vertical banks. At the Hoffman Creek site, the intermediate diameters of at least 100 randomly chosen bed particles were measured at several locations along the profile (Wolman, 1954).

4. Relief and gradient at the debris-flow–fluvial transition

Stream gradients (plotted vs. contributing area) of Bear and Cedar Creeks are "bedrock" channels according to the bedrock–alluvial discriminant found by Montgomery et al. (2003b) for their Knowles Creek study area, while gradients of Hoffman Creek are "alluvial" (Fig. 3) (note that Bear Creek is tributary to Knowles Creek within the Montgomery et al., 2003b, study reach). According to this discriminant, Hoffman Creek would be alluvial even without the many observed debris dams and their associated impoundments, but Bear and Cedar Creeks would be bedrock without those dams. Bear Creek is indeed predominantly a bedrock channel, including at the basin outlet, but Cedar Creek is predominantly alluvial, presumably due to debris-dam impoundments—the channel downstream of the outlet, past a large debris dam, is bedrock.

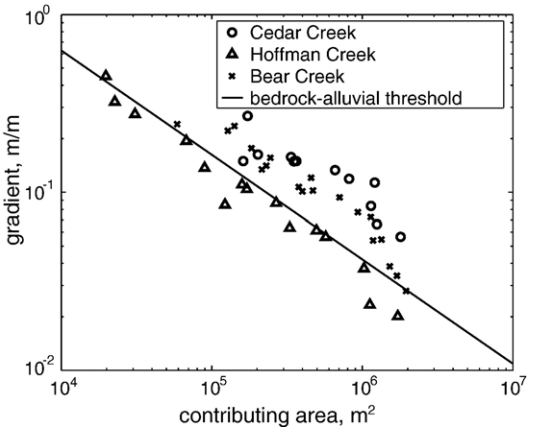

Fig. 3. Log–log plot of stream gradient vs. contributing area for Cedar Creek (circles), Hoffman Creek (triangles), and Bear Creek (×'s) sites surveyed in summer, 2000. Also shown is Montgomery et al.'s (2003b) bedrock–alluvial discriminant for their Knowles Creek study reach, which includes the Bear Creek confluence.

Field observations indicate that aggradation associated with Holocene sea-level rise extended to the Hoffman Creek outlet at 10 m above sea level and likely well upstream of that point. The lowest bedrock exposure in Hoffman Creek was found at the bottom of a scour pool 540 m upstream of, and 10 m above, the outlet. Below that point, gravel typically formed only a veneer of a few tens of centimeters over indurated, fine sediments. Gradients of Hoffman Creek, then, are likely limited by transport capacity or competence and indicative of declining topography.

While the longitudinal profiles of Bear and Cedar Creeks appear bedrock controlled, debris dams in these channels and in Hoffman Creek account for significant fractions of surveyed profile relief (Figs. 4 and 5). If such dams are typical, then at any given time, they comprise significant fractions of apparent profile relief of these and similar streams and result in shielding of significant portions of the bedrock by impounded alluvium. At the time of survey, bedrock exposure was limited to a few patches in Cedar Creek. While the bedrock profile was exposed at the upstream ends of the surveyed reaches and therefore spans the relief represented by the debris dams, these dams and their impounded sediment form much of the bed substrate and therefore dissipate much of the energy that might otherwise be dissipated by bedrock erosion.

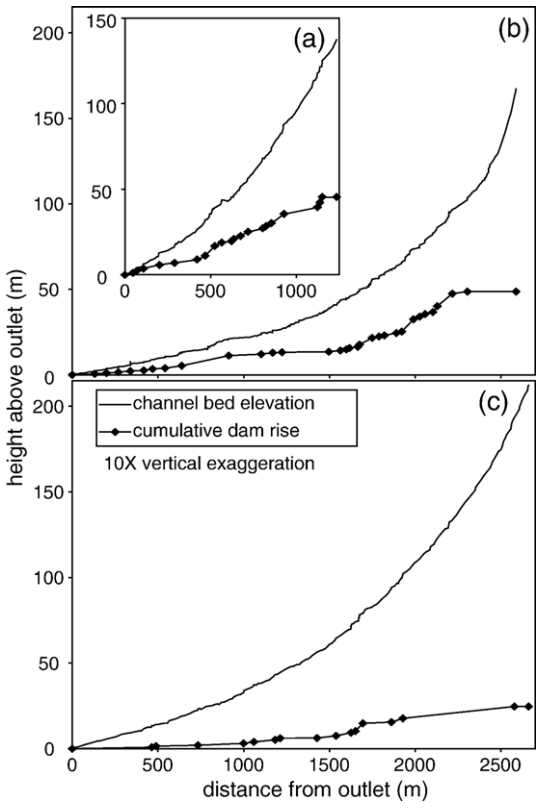

Fig. 4. Longitudinal profiles and cumulative relief of dams vs. distance from the outlets for (a) Cedar Creek, (b) Hoffman Creek, and (c) Bear Creek sites surveyed in summer 2000. Vertical exaggeration is 10 times.

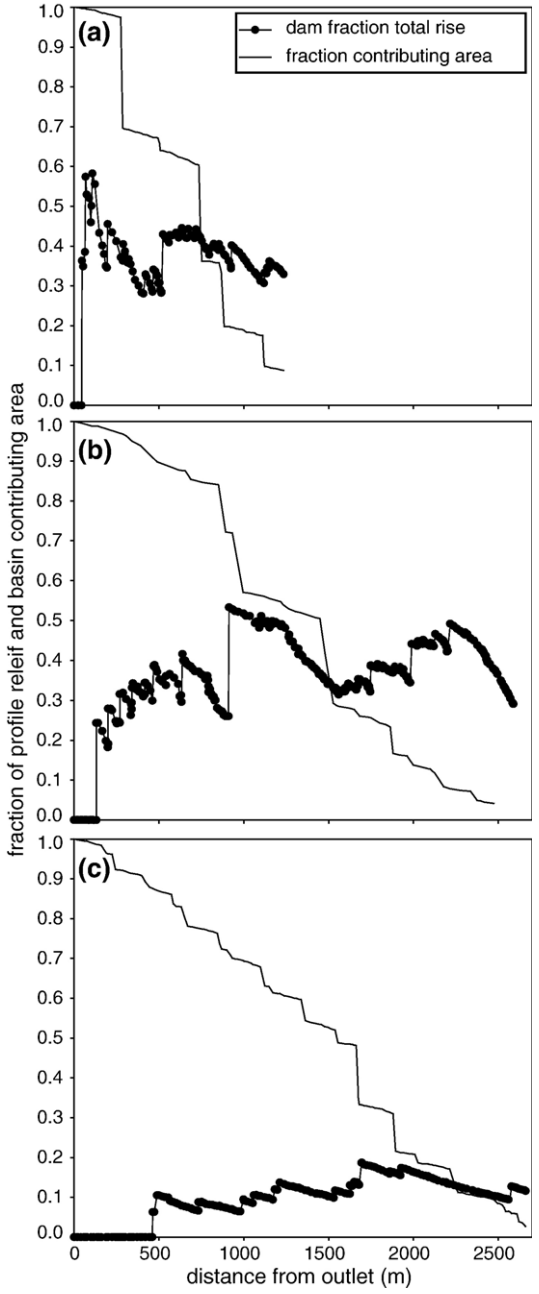

Fig. 5. Cumulative relief of dams as a fraction of total profile relief and contributing area as a fraction of the value at the outlet vs. distance upstream from the outlets for (a) Cedar Creek, (b) Hoffman Creek, and (c) Bear Creek sites surveyed in summer 2000.

Conceptually, then, relief of such streams consists of three components: debris dams, sediment impounded behind debris dams, and exposed bedrock. Similarly, stream gradients consist of three components:

$$S = S_d + S_a + S_r, \quad (1)$$

where S is stream gradient; S_d is gradient due to debris dams; S_a is gradient due to impounded alluvium; and S_r is gradient due to bedrock properties. A complete model of these streams should include, for each component, (a) the magnitude of its contribution to profile relief and gradient; (b) the mechanism for that contribution; and (c) the controls on its magnitude and distribution. These contributions are intertwined because the debris dams and impounded alluvium sit atop the bedrock and simply affect when that bedrock is exposed to erosive tools in the stream. The conceptual model of Eq. (1) is a starting point, then, for analyzing contributions to relief and gradient of the streams in the study basins and other streams like them. From an analysis of these component contributions, a more rigorous model is developed that incorporates their effects on bedrock erosion rate in headwater streams at the debris-flow–fluvial transition.

5. Relief and gradient of debris dams

Dam relief was summed along the longitudinal channel profile (Fig. 4), and these sums were divided by total profile relief at each point to show dam relief as a fraction of total profile relief (Fig. 5). The surveyed profiles are visibly stepped, and although steps in bedrock and indurated sediments do exist, debris dams account for most visible steps and large fractions of profile relief (Figs. 4 and 5). The maximum debris-dam relief fraction is greater by a factor of three in Cedar and Hoffman Creeks than in Bear Creek. The maximum relief fraction for all sites is 0.58 at 108 m from the outlet of Cedar Creek. The debris-dam relief fractions for the entire, surveyed profiles are 0.33, 0.29, and 0.12 for Cedar, Hoffman, and Bear Creeks, respectively, although these values are dependent on the upstream extents of the surveys—if the Hoffman Creek survey had been terminated at just over 80 m from the top of the last dam, as the surveys for Cedar and Bear Creeks were, the dam relief fraction for the surveyed profile would instead be 0.43. The surveyed dam relief accounts for 9.8%, 19%, and 6.4% of total basin relief for Cedar, Hoffman, and Bear Creeks, respectively. According to these results, debris dams alone make significant contributions to relief in the study basins.

Dam relief is neither uniformly distributed along the profiles nor always proportional to local profile gradient, and the relative locations of the relief-fraction maxima vary among sites (Figs. 4 and 5). That maximum is near Cedar Creek's outlet, near the middle of the Hoffman Creek profile, and further upstream for Bear Creek. Visual inspection of the basin maps (Fig. 1) and Figs. 4 and 5 suggests that locations of relief-fraction maxima are related to "proximal" upstream network structure with a high bifurcation ratio (i.e., degree of branching), although that proximity is likely measured in terms of high (but not too high) gradients and low tributary junction angles rather than short horizontal distances (Benda and Cundy, 1990; Lancaster et al., 2001, 2003; Daniel J. Miller and Kelly Burnett, personal communication, 2003). In the steepest, upstream-most parts of the profiles, accumulation of relief in debris dams is relatively small because debris flows often scour and rarely deposit there. The steepest parts of the cumulative dam relief profiles are downstream of these steepest channel reaches, in reaches that are prone to debris flows but where debris-flow deposition rather than scour predominates. Further downstream, gradients are lower, debris flow sources are generally limited to tributaries rather than upstream along the main stem, and gradients of the cumulative dam relief profiles decrease.

These trends are evident in distributions of dam height-to-spacing ratio–essentially gradient due to debris dams, S_d–with respect to contributing area at the downstream dam (Fig. 6). Points at the smallest contributing areas indicate locations of the second

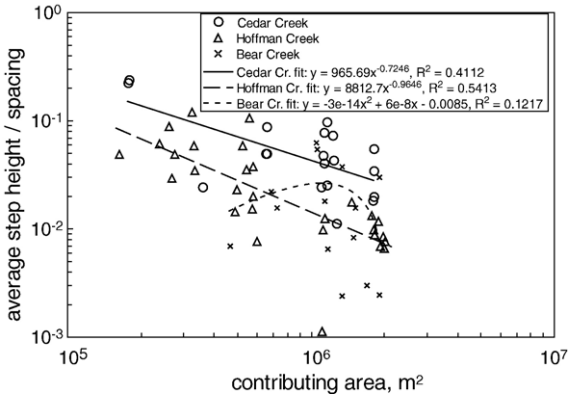

Fig. 6. Log–log plot of dam height-to-spacing ratio (average height of two adjacent dams divided by the horizontal distance between them) vs. contributing area at the downstream dam for Cedar Creek (circles), Hoffman Creek (triangles), and Bear Creek (×'s) sites surveyed in summer, 2000; power-law fit to Cedar and Hoffman Creek data; and polynomial fit to Bear Creek data.

debris dams in the downstream direction, found at contributing areas of 0.1–0.2 km^2 for Cedar and Hoffman Creeks and of 0.5 km^2 for Bear Creek (1200 m, 2100 m, and 1900 m from the outlet for Cedar, Hoffman, and Bear Creeks, respectively; Fig. 5). Height-to-spacing ratios are dependent on events with great inherent stochasticity, i.e., debris-flow deposition and, to a lesser extent, trees falling and therefore expected to vary in space and time. Still, for Hoffman Creek the relationship between the height-to-spacing ratio and contributing area is relatively strong such that a negative-power law of contributing area describes 54% of the variance in the dam height-to-spacing ratio (Fig. 6). A negative-power–law relationship also fits the Cedar Creek data relatively well (R^2=41%). That is, for these channels, the dam height-to-spacing ratio generally decreases with contributing area. For Bear Creek a humped function with a peak at ~1 km^2 is a weak fit to the data (R^2=12%). It is likely that dam formation in Bear Creek is more strongly related to trees falling into the stream than to debris-flow deposition, as in the other streams, because large (DBH>1–2 m) conifers comprise much of the riparian forest and indicate a long time since large, debris-flow-generating disturbance (e.g., clear-cut timber harvest, forest fire). If more dams are due to trees falling, a process unrelated to network structure, then the relationship between dam height-to-spacing ratio and contributing area should be weak.

6. Gradient of impounded alluvium

While the data show that debris dams comprise significant fractions of relief of all profiles, visual inspection of Fig. 4 indicates that significant relief is also attributable to alluvium impounded behind those dams. Measuring that relief in the field is infeasible because attributing alluviation in particular locations with particular dams is difficult, especially where alluviated reaches overlap or are superimposed—debris flows frequently deposit on older deposits (Lancaster et al., 2003). It is necessary therefore, to seek an analytical expression for alluvial gradient, S_a, that, when coupled with observed distributions of debris dams, will allow estimation of impoundments' effect on profile relief.

Debris dams cause impoundment of sediment and, therefore, local alluviation because the logs and/or boulders comprising the dams provide less erodible, local, base-level controls. Channel beds in these impounded reaches have gradients lower than average valley gradients, a fact that indicates that these steeper valley gradients are not controlled by critical shear stress for bedload transport, although gradients in impounded, alluviated reaches probably are so controlled.

To find an expression for gradient in these alluviated reaches, S_a, it was assumed that such gradients are governed by the critical shear stress for initiation of particle motion (rather than, say, transport capacity) at bankfull discharge, as in Stock et al. (2005). That is, impoundments fill with sediment until alluviated gradients reach the threshold for initiation of particle motion. Any more filling results in steeper gradients and therefore degradation due to excess transport capacity. Assuming bed shear stresses in impounded reaches are well approximated by the assumption of steady, uniform flow–a fair assumption for many of the apparently graded impoundments observed in the field (Fig. 2)–gradient is related to critical dimensionless shear stress,

$$\tau_c* = \frac{hS_a}{(s-1)D} \tag{2}$$

where h is bankfull flow depth and assumed approximately equal to hydraulic radius under the wide-channel assumption; s is ratio of particle to fluid density; and D is the relevant grain diameter, e.g., D_{84}. Solving for gradient,

$$S_a = \frac{(s-1)D\tau_c*}{h}. \tag{3}$$

To find flow depth, the Manning equation and continuity principle are used to obtain

$$Q = \frac{h^{5/3}S_a^{1/2}}{n_m}b_c, \tag{4}$$

where Q is bankfull discharge; b_c is channel width; and n_m is the Manning roughness number. Substituting hydraulic geometry relationships, $Q=k_Q A^{m_q}$ and $b_c=k_b A^c$, and solving for flow depth, h,

$$h = k_Q^{3/5} n^{3/5} k_b^{-3/5} A^{3(m_q-c)/5} S^{-3/10}, \tag{5}$$

and substituting Eqs. (5) into (3),

$$S_a = K_a A^{-\theta_a} \tag{6}$$

with

$$K_a = [(s-1)D\tau_c*]^{10/7}\left(\frac{k_b}{k_Q n_m}\right)^{6/7} \tag{7}$$

and

$$\theta_a = 6(m_q-c)/7, \tag{8}$$

where Eqs. (6)–(8) are similar to expressions derived by Stock et al. (2005).

Table 2
Parameters, values, and sources

Parameter	Value	Source[a]
k_b, c	1.87×10^{-2} m^{1-2c}, 0.389	AS
D_{84}	8.7×10^{-2} m	HC
τ_c*	0.05	Assumed
s	2.0	Various[b]
n_m	0.11	Estimated
k_Q, m_q	1×10^{-5} m^{3-2m_q}/s, 0.8	Estimated, assumed
K_a, θ_a	1.8, 0.35	Calculated
b_c/b_v	0.213	AS
ε	10^{-4} m/year	Various[c]
K	10^{-5} $year^{-1}$	Estimated
m, n	0.5, 1.0	Assumed

[a] AS=data from all sites; HC=data from Hoffman Creek site.
[b] e.g., Reneau and Dietrich (1991); Heimsath et al. (2001); Anderson et al. (2002).
[c] e.g., Reneau and Dietrich (1991); Personius et al. (1993); Heimsath et al. (2001).

Stock et al. (2005) hypothesized that, if valley gradients were controlled by critical shear stress, downstream fining might be responsible for some profile concavity. In the present derivation of S_a, grain diameter, D, is included in the constant, K_a (Eq. (7)), because pebble counts in Hoffman Creek revealed no discernible trends in grain sizes with respect to contributing area or distance from the basin outlet and, while pebble counts were not made in Cedar and Bear Creeks, channel bed observations and photographs at many locations along these streams are consistent with the Hoffman Creek results. Despite the lack of downstream fining, alluvial gradients still contribute to profile concavity. The power-law fit to measured values of incised channel width (b_c) vs. contributing area (A) for all sites is $b_c=(1.87\times10^{-2})A^{0.389}$ ($R^2=0.4205$), i.e., $c=0.389$. Assuming a typical value of $m_q=0.8$, $\theta_a=0.35$ (Table 2). Downstream changes in alluvial gradient, however, are not great enough to explain all of the observed profile concavity, i.e., for all the sites, $\theta>0.35$ in power-law fits to slope-area trends, $S\propto A^{-\theta}$, where S is stream gradient and A is contributing area (Fig. 3, Table 1).

7. Bedrock erosion and a unified model of profile relief and gradient

The predominance of debris dams and associated bedrock shielding by impounded sediment must exert some control on long-term incision rates and, therefore, gradient and total profile relief. Montgomery et al. (2003a) reasoned that relatively immobile wood must inevitably steepen stream profiles. Here an attempt is made to quantify that effect.

Stock et al. (2005) found that short-term (1–5 years) bedrock incision rates are much greater than long-term average bedrock lowering rates and argued that longitudinal profiles were governed by the critical shear stress for gravel entrainment rather than bedrock erodibility. Observations in this study indicate that bedrock shielding, both by valley-floor deposits outside the channel (Lancaster et al., 2001; Casebeer, 2004) and impounded sediment within the channel, is a more plausible explanation of these rapid incision rates. Because the eroding bedrock surface is often shielded, the channel must erode the bedrock, when it is exposed, more quickly than the average rate in order to keep up with long-term lowering rates.

Fluvial erosion at a point on the valley bottom occurs if and only if (a) the sediment thickness is zero (or negligible) and (b) the channel, which in the study areas is almost always much narrower than the valley bottom, currently "visits" that point. Here a bedrock erosion rate is assumed, ε, that follows the "stream-power" law when bedrock is exposed:

$$\varepsilon = P_{lat}P_{ver}KA^mS^n, \tag{9}$$

where P_{lat} $(0\le P_{lat}\le 1)$ is the probability that the channel is at a given point along the valley-bottom cross-section; P_{ver} $(0\le P_{ver}\le 1)$ is the probability of bedrock exposure in the channel bed; K is a coefficient encompassing hydraulic erosivity and bedrock erodibility (e.g., Whipple and Tucker, 1999, 2002); A is contributing area; S is stream gradient; and m and n are exponents depending on hydraulic geometry and detachment process (Whipple and Tucker, 1999), e.g., $m=0.3$, $n=0.7$ for erosion proportional to shear stress, and $m=0.5$, $n=1.0$ for erosion proportional to unit stream power. For lowering over a valley cross-section, contributing area, A, applies to that whole cross-section. Note that P_{lat} and P_{ver} decrease the effective, long-term erosivity/erodibility coefficient.

Stock and Dietrich (2003) argued that debris flows, rather than fluvial processes, dominate bedrock erosion in channels with gradients >0.1 and curved trends of stream gradient vs. contributing area (slope-area) signify this debris-flow–dominated scour, but we use a stream-power law in Eq. (9). While the slope-area trends for Cedar and Bear Creeks may be curved (the Cedar Creek data are ambiguous), the Cedar and Bear Creek sites have large debris-flow deposits and associated dams at gradients >0.1. (For Bear Creek, gradients are <0.1 at contributing area >0.7 km^2, or >0.3 of the basin total. For Cedar Creek, gradients are <0.1 at contributing

area >1 km^2, or >0.5 of the basin total (Figs. 3–5)). Moreover, the valleys have flat bedrock bottoms, which might be inferred as owing to continual lateral migration due to avulsion and, therefore, signatures of frequent deposition rather than scour. While deposits and flat valley bottoms do not exclude episodic scour by debris flows, especially in reaches with gradients greater than ~0.1, we infer dominance of fluvial erosion in valleys with these features.

The probability, P_{lat}, can be represented by the ratio of channel to valley width, or

$$P_{lat} = \frac{b_c}{b_v} \tag{10}$$

where b_v is the valley width. Measurements of incised channel and valley widths reveal trends of channel width with contributing area but not of the ratio of channel to valley width. Of course, channel width varies spatially and temporally, and valley width varies spatially—also temporally for long times. This variability is apparent in the data, but trends with contributing area are not. Linear and power-law fits (not shown) against both contributing area and distance downstream all have $R^2 \leq 0.01$. The average b_c/b_v value is relatively consistent among sites: 0.198 for Hoffman Cr.; 0.248 for Bear Cr.; and 0.191 for Cedar Cr.; all similar to the average of all the data, $\overline{(b_c/b_v)} = 0.213$.

To find the probability, P_{ver}, that the channel bed is exposed, it is first necessary to find the probability that the bed is covered with sediment by finding the fractional coverage due to impoundments. Assumptions are as follows. (1) Channel aggradation occurs if and only if forced by impoundment behind debris dams. According to Fig. 3, this is a good assumption for Cedar and Bear Creeks but not for Hoffman Creek. (2) Dam formation is stochastic such that, at any point along a given reach, the ratio of dam height to spacing is a random variable with a well defined mean. The inherent variability of debris-dam formation is recognized (Benda and Dunne, 1997; Lancaster et al., 2001), as is the controlling influence of local network structure (Benda and Cundy, 1990; Benda and Dunne, 1997; Lancaster et al., 2001, 2003; Benda et al., 2003). Dams formed by riparian tree-fall likely superimpose a nearly uniform randomness (Robison and Beschta, 1990; Van Sickle and Gregory, 1990). (3) Grade control by debris dams is instantaneous, i.e., impoundments fill instantaneously, and channel lowering follows dam lowering without delay. In Hoffman Creek, it is deduced that impoundments extending a few tens of meters and over 100 m upstream, respectively, filled in less than 3 years. Although indurated deposits can resist incision, most alluvial reaches appear graded to debris dams. In Cedar Creek, downstream of the study site, the channel evacuated 1–2 m of alluvium to expose bedrock in less than a year following debris-dam removal. Such times are small with respect to the lifetime of an individual dam, e.g., 50–100 years (Hogan et al., 1998) and effectively instantaneous with respect to the timescales of denudation and longitudinal channel profile evolution in the Oregon Coast Range, where denudation and incision rates are typically 0.1 mm/year (e.g., Reneau and Dietrich, 1991; Personius, 1995; Heimsath et al., 2001). (4) Dams have negligible streamwise thickness. This assumption might lead to underestimation of bed shielding because many debris dams have substantial streamwise thickness (Fig. 2b), but the importance of such thickness is unclear, and its inclusion would substantially complicate the model.

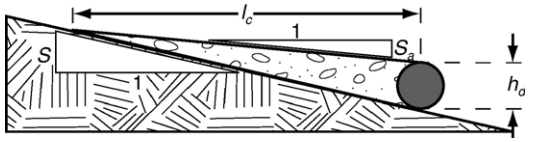

Fig. 7. Schematic of dam of height (h_d); impounded, alluviated reach upstream with length (l_c), and surface gradient (S_a) on underlying bedrock surface with gradient (S).

To find streamwise length of sediment impounded behind a dam of a given height, h_d, note that rise due to the dam and associated impoundment must equal rise of the underlying bedrock profile over the same distance, or

$$h_d + S_a l_c = S l_c. \tag{11}$$

where alluvial gradient, S_a, is given by Eqs. (6)–(8); l_c is horizontal impoundment length; and S is average valley gradient, i.e., gradient of the underlying bedrock surface (Fig. 7). Solving Eq. (11) for impoundment length, then

$$l_c = \frac{h_d}{S - S_a}. \tag{12}$$

For a given reach of length, L, the total length of impoundments is the sum of the N individual lengths, i.e.,

$$L_c = \frac{1}{S - S_a} \sum_{i=1}^{N} h_{d_i}. \tag{13}$$

Using h_d to represent the average dam height for the reach, then

$$L_c = \frac{N h_d}{S - S_a}. \tag{14}$$

For fractional bed coverage, L_c/L, Eq. (14) is divided by total reach length, L. The ratio L/N is the average dam spacing, which is represented as λ. The probability of bedrock exposure is then one minus the fractional bed coverage, or

$$P_{ver} = 1 - \frac{h_d}{\lambda(S - S_a)}, \quad 0 \le P_{ver} \le 1. \tag{15}$$

The condition, $0 \le P_{ver} \le 1$, means that (a) $S > S_a$ and (b) $S \ge h_d/\lambda + S_a$. The latter, more strict condition states that average gradient must be greater than or equal to the sum of alluvial gradient and gradient due to debris dams and is essentially equivalent to Eq. (11). This condition is also equivalent to requiring that total length of impoundments in a reach cannot exceed reach length. Explicit accounting for overlapping of sediment impoundments is neglected herein. This neglect may result in overestimation of bed coverage and, consequently, overestimation of the overall slope, although the condition of Eq. (15) limits that overestimate.

Substituting with Eqs. (6), (10), and (15) in Eq. (9), the long-term incision rate is expressed as

$$\varepsilon = \frac{b_c}{b_v}\left[1 - \frac{h_d}{\lambda(S - K_a A^{-\theta_a})}\right] K A^m S^n. \tag{16}$$

For the special case of $n = 1$ (e.g., for incision of uncovered bedrock proportional to unit stream power), Eq. (16) is quadratic with respect to gradient, S. The condition of Eq. (15) disallows the smaller solution, so

$$S = \frac{1}{2}(S_d + S_a + S_r) + \sqrt{\frac{1}{4}\left(S_d + S_a + S_r\right)^2 - S_a S_r} \tag{17}$$

for

$$S_d = \frac{h_d}{\lambda}, \tag{18}$$

$$S_r = \frac{\varepsilon}{K}\left(\frac{b_c}{b_v}\right)^{-1} A^{-m}, \tag{19}$$

and S_a given by Eq. (6). Eq. (17) predicts the valley gradient for steady-state incision of the underlying bedrock and is similar to the conceptual model, Eq. (1). The condition of Eq. (15) gives a minimum gradient applicable to an aggrading valley,

$$S_{min} = S_d + S_a. \tag{20}$$

Gradients were calculated with Eqs. (6) and (17)–(20), parameters from the field sites (Table 2), and the fit between h_d/λ and contributing area for Hoffman Creek (Fig. 6) and plotted with the observed gradients from all three sites in Fig. 8. Bedrock erodibility was estimated based on denudation rates found in the Oregon Coast Range (Reneau and Dietrich, 1991; Heimsath et al., 2001) and the finding of Stock et al. (2005) that rates of erosion of unshielded bedrock are typically greater than long-term denudation rates by an order of magnitude or more. The observed Hoffman Creek gradients, which fall below the bedrock-alluvial discriminant of Montgomery et al. (2003b), are similar to the S_{min} values calculated with Eq. (20). Cedar and Bear Creek gradients, on the "bedrock" side of the discriminant, are similar to the predicted bedrock gradients, S, calculated from Eq. (17). Fits to h_d/λ vs. A for Cedar and Bear Creeks, respectively (Fig. 6), are used to calculate gradients with Eq. (17) and are shown with observed gradients at the respective sites in Fig. 9.

Among the three sites, bedrock gradients are best predicted in Cedar Creek—Hoffman Creek gradients are not expected to approach predicted bedrock gradients, and Bear Creek has a weak relationship between h_d/λ and contributing area. For Cedar Creek, then, the "predicted" longitudinal profiles with and without the influence of dams (i.e., with S from Eq. (17) and S_r from Eq. (19), respectively) are particularly illustrative when compared to the surveyed profile (Fig. 10). Comparison of the two model profiles indicates that

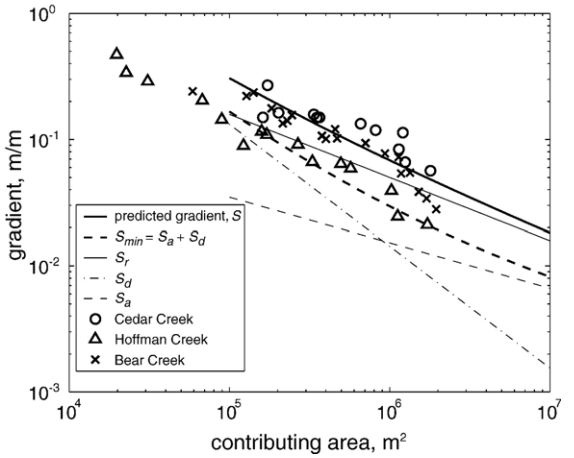

Fig. 8. Calculated (with parameters from Table 2) and observed relationships between gradient and contributing area. Gradient, S (heavy solid line), from Eq. (17) represents predicted valley gradient for a steady valley incision rate. S_{min} (heavy dashed line), from Eq. (20), is the predicted minimum gradient given the observed and predicted dependencies of debris dam, S_d, and alluvial gradients, S_a, respectively, on contributing area. "Bedrock," dam, and alluvial gradients, S_r, S_d, and S_a, respectively (from Eqs. (19), (18), and (6), respectively), are shown (thinner lines) for reference.

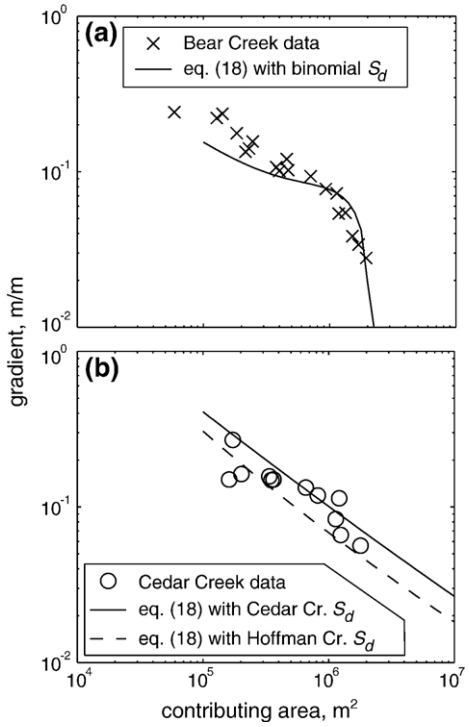

Fig. 9. Calculated and observed relationships between gradient and contributing area for (a) Bear Creek and (b) Cedar Creek. Valley gradient, S (heavy solid line), is calculated with Eq. (17) and S_d from the binomial (a) and power-law (b) fits to the h_d/λ vs. A data from Bear and Cedar Creeks, respectively (Fig. 6). In (b), the gradient calculated with the power-law fit to the h_d/λ vs. A data from Hoffman Creek (and also shown in Fig. 8) is shown for comparison (lighter dashed line).

55% of the predicted total profile relief is due to dams and associated impoundments (Fig. 10), an amount significantly larger than the observed 33% attributable to dams alone (Fig. 5). It appears, then, that a significant fraction of dam-related relief, perhaps 40%, is due to impounded alluvium.

8. Discussion

While the apparent predictive capacity of the model is substantial, most notably for the Cedar and Hoffman Creek sites, this capacity is not surprising, nor does the utility of the model rest entirely on its predictive capacity. At base, the model illustrates the effects of persistent bed shielding on the evolution of mountain streams incising bedrock. As an illustrative model, it is generalizable to any bedrock stream in which persistent debris dams form. Of course, some debris dams, such as those formed by high-volume, deep-seated landslides, are much bigger than those studied here, and large size can reduce the applicability of some of the assumptions. For example, Triangle Lake, in the Oregon Coast Range, was formed by a deep-seated landslide >40 ka (Worona and Whitlock, 1995). Triangle Lake's continued existence is evidence that the assumption of instantaneous filling with sediment is not applicable in this case. Still, the following results apply: (a) Any incising stream will steepen in response to persistent, substantial bed coverage by impounded sediment, and (b) this steepening is dependent on the spatial and temporal distribution of debris dams. The conceptual and analytical model presented here provides a framework with which to address the effects of debris dams on longitudinal channel profile evolution in general and for other specific cases.

Even with the necessary caveats, the agreements between predicted and observed gradients and longitudinal profiles are, on the one hand, remarkable, especially given that the model was not calibrated—parameters were estimated from quantitative data, but no parameters were "tuned" to give the desired result. On the other hand, the model has a firm basis in data and ineluctable geometry. Perhaps more surprising than the final "products" are the good power-law fits to the observed relationships between step height-to-spacing ratio and contributing area for Cedar and Hoffman Creeks. Given those good fits and the other data, the ability of the model to predict reasonable slopes for these basins is perhaps less remarkable.

In general, the component of gradient due to debris dams, S_d, changes in a complicated way downstream, likely because the probability of debris-flow deposition, the primary dam-forming agent, changes in a complicated way downstream and depends on, for example, the sizes of and the spacings between tributaries (e.g.,

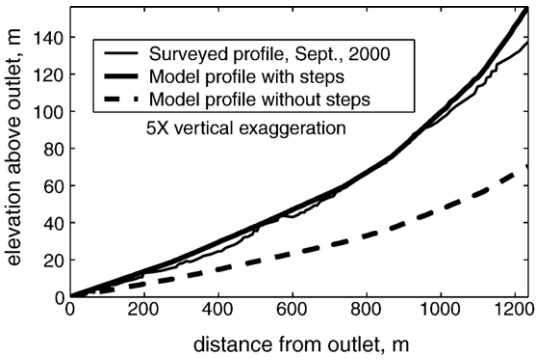

Fig. 10. Surveyed and model longitudinal profiles for Cedar Creek. Model profiles are calculated with DEM-derived contributing areas at surveyed locations. Model profile with debris dams is calculated with gradient, S, from Eq. (17) and S_d from the Cedar Creek site fit (Fig. 6), as in Fig. 9. Model profile without dams is calculated with gradient, S_r, from Eq. (19).

Benda and Cundy, 1990; Lancaster et al., 2001, 2003; Benda et al., 2003). In the leaf-shaped Hoffman Creek basin (Fig. 1), the trend of fewer debris-flow–delivering tributaries downstream (Fig. 5) likely contributes not only to the strong relationship between h_d/λ and contributing area (Fig. 6) but also to the nearly power-law decline in stream gradients with increasing contributing area (Fig. 3). In contrast, the transition between leaf-shaped and trellis-shaped network structures in the upper and lower halves, respectively, of Bear Creek (Fig. 1) and the corresponding lack of major tributaries <1500 m from the outlet (Fig. 5) correspond to the peak in h_d/λ at $A=10^6$ m^2 and its steep decline downstream (Fig. 6). While the binomial fit in Fig. 6 explains little of the variance in dam height-to-spacing ratio, using that fit in Eq. (17) is illustrative of the implications of such a humped function: a change to greater profile concavity at contributing areas $>10^6$ m^2, similar to the kind of change observed in the slope–area data (Fig. 9). In the heart-shaped Cedar Creek basin (Fig. 1), the relatively closer proximity to larger tributaries along the whole profile (Fig. 5) likely contributes not only to the more gradual decline in h_d/λ with contributing area (Fig. 6) but also to larger gradients and lower profile concavity, consistent with the prediction of Eq. (17) (Fig. 9).

Different network structures among the sites and seemingly consistent differences in the spatial distributions of h_d/λ suggest a linkage between network structure and h_d/λ and, therefore, valley gradient, but different histories of land use could also explain differences in h_d/λ among the study sites, and the data presented here may not be representative of long-term temporal average conditions. In the Bear Creek basin, aside from recent clear-cuts in the headwaters (>2000 m from the outlet) and near the outlet (<400 m from the outlet), much of the basin is forested with old growth, and some riparian conifers have diameters >2 m. In contrast, the Hoffman and Cedar Creek basins have complicated harvest and fire histories involving substantial recent clear-cuts (Swanson et al., 1977; Lancaster et al., 2001, 2003). The long-term temporal average relief of debris dams in any of the study basins is likely less than that in Hoffman and Cedar Creeks but greater than that in Bear Creek. While their different histories likely explain the greater observed dam relief in the Hoffman and Cedar sites, the different spatial distributions of dams are not obviously related to those different histories. Still, while different network structures remain a likely explanation for those different distributions, the linkage cannot be conclusively demonstrated, for example, without replication of similar associations between dam distribution and network structure in many sites.

The field data and the model presented above indicate that all three components of gradient and relief considered here are important. While neither the dam relief nor that of the impounded alluvium are independent of the underlying bedrock profile, they do impose significant requirements on profile gradients in order that fluvial processes erode bedrock in spite of shielding by debris dams and their impounded sediment. Whipple and Tucker (1999, 2002) showed that the condition of steady state between relative rock uplift (or declining base level) and fluvial incision could be used to evaluate gradients of mountain streams. While such a steady state may be an ideal never quite attained, it is a useful reference in the Oregon Coast Range, where denudation rates, sediment yields, and stream incision rates are approximately equivalent in areas similar to the present field sites (e.g., Reneau and Dietrich, 1991; Personius, 1995). The applicable lesson is that, given continued tectonic input of material via rock uplift (or, effectively, by declining base level), gradients will necessarily increase until denudational and erosional processes are capable of removing that input. In the Oregon Coast Range, and in the study sites specifically, debris flows and tree-fall deliver to streams materials that result in substantial shielding of the bedrock at any given time. In this area of active rock uplift, the streams steepen until they can both remove those materials and erode the underlying bedrock. Spatial and temporal controls on the formation and persistence of debris dams are, therefore, also controls on bedrock erosion, stream gradient, and basin relief.

9. Conclusion

Field data from surveyed longitudinal profiles of the main channels of three small (~2 km^2) watersheds in the Oregon Coast Range, USA, show that wood and boulder dams comprise significant fractions of total surveyed relief for each profile–33%, 29%, and 12% for the Cedar, Hoffman, and Bear Creek sites, respectively–and up to 58% at one location along the Cedar Creek profile.

A model of the relationship between valley gradient and contributing area shows that both the dams and the alluviation of reaches impounded by those dams have significant effects on gradient and, thus, profile relief. At the Cedar Creek site, calculations of the profile with the observed relationship between the dam height-to-spacing ratio and contributing area indicate that ~20% of the total profile relief may be due to such alluviation.

This model and the data suggest that network structure, by controlling the susceptibility of different parts of the main valley to debris-flow deposition and, thus, debris-dam formation, has a significant effect on the shape of the profile, although that effect is not conclusively demonstrated here. Still, where the dam height-to-spacing ratio falls steeply, possibly due to a change in network structure, profile concavity also increases, i.e., valley gradient also falls more steeply with greater contributing area.

The results of this study show that a significant fraction of the relief of forested, mountain landscapes typified by the field sites in the Oregon Coast Range, USA, is due to the effects of relatively immobile wood and boulders deposited in the valleys by debris flows.

Acknowledgements

This research was funded in part by the CLAMS Project, Pacific Northwest Research Station, USDA Forest Service. Shannon Hayes, John Green, Simon Mudd, Christine May, and Robin Beebee assisted with field work. Adam Kent provided some insight into the bedrock geology of the Oregon Coast Range. Steve Darby and Paul Carling provided helpful reviews.

Appendix A. List of symbols

A	contributing area
b_c	channel width
b_v	valley width
c	exponent in relationship between channel width and contributing area
D	grain diameter
h	bankfull flow depth
h_d	dam height
K	coefficient in stream-power erosion law
K_a	coefficient in relationship between alluvial gradient and contributing area
k_b	coefficient in relationship between channel width and contributing area
k_Q	coefficient in relationship between discharge and contributing area
L	reach length
L_c	total length covered by impoundments in reach
l_c	impoundment length
m	exponent on contributing area, A, in stream-power law
m_q	exponent in relationship between discharge and contributing area
N	number of impoundments in a reach
n	exponent on stream gradient, S, in stream-power law
n_m	Manning roughness
P_{lat}	probability that channel is at a given lateral location
P_{ver}	probability of bedrock exposure in channel bed
Q	bankfull discharge
S	stream or valley gradient
S_a	alluvial gradient
S_r	gradient due to bedrock erosion alone
S_{min}	minimum valley gradient for aggrading profile, S_d+S_a
S_d	dam gradient, or ratio of dam height to spacing, h_d/λ
s	ratio of particle to fluid density
β	steepness index
ε	bedrock erosion rate
θ	concavity index
θ_a	exponent in relationship between alluvial gradient and contributing area
λ	average dam spacing, L/N
τ_c^*	critical dimensionless shear stress

References

Anderson, S.P., Dietrich, W.E., Brimhall Jr., G.H., 2002. Weathering profiles, mass-balance analysis, and rates of solute loss: linkages between weathering and erosion in a small, steep catchment. Geol. Soc. Amer. Bull. 114 (9), 1143–1158.

Benda, L.E., 1990. The influence of debris flows on channels and valley floors in the Oregon Coast Range, USA. Earth Surf. Process. Landf. 15 (5), 457–466.

Benda, L.E., Cundy, T.W., 1990. Predicting deposition of debris flows in mountain channels. Can. Geotech. J. 27 (4), 409–417.

Benda, L., Dunne, T., 1997. Stochastic forcing of sediment supply to channel networks from landsliding and debris flow. Water Resour. Res. 33 (12), 2849–2863.

Benda, L., Veldhuisen, C., Black, J., 2003. Debris flows as agents of morphological heterogeneity at low-order confluences, Olympic Mountains, Washington. Geol. Soc. Amer. Bull. 115 (9), 1110–1121.

Buffington, J.M., Lisle, T.E., Woodsmith, R.D., Hilton, S., 2002. Controls on the size and occurrence of pools in coarse-grained forest rivers. River Res. Appl. 18 (6), 507–531.

Casebeer, N.E., 2004. Sediment storage in a headwater valley of the Oregon Coast Range: erosion rates and styles and valley-floor capacitance. M.S. Thesis, 48 pp., Oregon State Univ., Corvallis.

Dietrich, W.E., Dunne, T., 1978. Sediment budget for a small catchment in mountainous terrain. Z. Geomorphol. 29, 191–206.

Duan, J., 1996. A coupled hydrologic–geomorphic model for evaluating effects of vegetation change on watersheds. PhD thesis, 133 pp., Oregon State Univ., Corvallis.

Eaton, L.S., Morgan, B.J., Kochel, R.C., Howard, A.D., 2003. Role of debris flows in long-term landscape denudation in the central Appalachians of Virginia. Geology 31 (4), 339–342.

Grier, C.C., Logan, R.S., 1977. Old-growth *Pseudotsuga menziesii* communities of a western Oregon watershed: biomass distribution and production budgets. Ecol. Monogr. 47, 373–400.

Heimsath, A.M., Dietrich, W.E., Nishiizumi, K., Finkel, R.C., 2001. Stochastic processes of soil production and transport: erosion rates, topographic variation, and cosmogenic nuclides in the Oregon Coast Range. Earth Surf. Process. Landf. 26, 531–552.

Hogan, D.L., Bird, S.A., Hassan, M.A., 1998. Spatial and temporal evolution of small coastal gravel-bed streams: influence of forest management on channel morphology and fish habitats. In: Klingeman, P.C., Beschta, R.L., Komar, P.D., Bradley, J.B. (Eds.), Gravel-Bed Rivers in the Environment. Water Resources Publications, Highlands Ranch, CO, pp. 365–392.

Hyatt, T.L., Naiman, R.J., 2001. The residence time of large woody debris in the Queets River, Washington, USA. Ecol. Appl. 11 (1), 191–202.

Lancaster, S.T., Hayes, S.K., Grant, G.E., 2001. Modeling sediment and wood storage and dynamics in small mountainous watersheds. In: Dorava, J.M., Montgomery, D.R., Palcsak, B.B., Fitzpatrick, F.A. (Eds.), Geomorphic Processes and Riverine Habitat. Water Sci. Appl., vol. 4. American Geophysical Union, Washington, DC, pp. 85–102.

Lancaster, S.T., Hayes, S.K., Grant, G.E., 2003. Effects of wood on debris flow runout in small mountain watersheds. Water Resour. Res. 39 (6), 1168. doi:10.1029/2001WR001227.

Marcus, W.A., Marston, R.A., Colvard Jr., C.R., Gray, R.D., 2002. Mapping the spatial and temporal distributions of woody debris in streams of the Greater Yellowstone Ecosystem, USA. Geomorphology 44, 323–335.

Marston, R.A., 1982. The geomorphic significance of log steps in forest streams. Ann. Assoc. Am. Geogr. 72 (1), 99–108.

Massong, T.M., Montgomery, D.R., 2000. Influence of sediment supply, lithology, and wood debris on the distribution of bedrock and alluvial channels. Geol. Soc. Amer. Bull. 112 (5), 591–599.

May, C.L., 2002. Debris flows through different forest age classes in the central Oregon Coast Range. J. Am. Water Resour. Assoc. 38 (4), 1097–1113.

May, C.L., Gresswell, R.E., 2003. Processes and rates of sediment and wood accumulation in headwater streams of the Oregon Coast Range, USA. Earth Surf. Process. Landf. 28, 409–424. doi:10.1002/esp.450.

Mayer, L., 1990. Introduction to Quantitative Geomorphology: An Exercise Manual. Prentice Hall, Englewood Cliffs, NJ. 380 pp.

Montgomery, D.R., Abbe, T.B., Buffington, J.M., Peterson, N.P., Schmidt, K.M., Stock, J.D., 1996. Distribution of bedrock and alluvial channels in forested mountain drainage basins. Nature 318, 587–589.

Montgomery, D.R., Collins, B.D., Buffington, J.M., Abbe, T.B., 2003a. Geomorphic effects of wood in rivers. In: Gregory, S.V., Boyer, K.L., Gurnell, A.M. (Eds.), The Ecology and Management of Wood in World Rivers. American Fisheries Society Symposium, vol. 37. American Fisheries Society, Bethesda, MD, pp. 21–48.

Montgomery, D.R., Massong, T.M., Hawley, S.C.S., 2003b. Influence of debris flows and log jams on the location of pools and alluvial channel reaches, Oregon Coast Range. Geol. Soc. Amer. Bull. 115 (1), 78–88.

Nakamura, F., Swanson, F.J., 1993. Effects of coarse woody debris on morphology and sediment storage of a mountain stream system in western Oregon. Earth Surf. Process. Landf. 18, 43–61.

Peck, D.L., 1961. Geologic map of Oregon west of the 121st Meridian. U.S. Geol. Surv. Misc. Geologic Investigations Map, I-325.

Personius, S.F., 1995. Late Quaternary stream incision and uplift in the forearc of the Cascadia subduction zone, western Oregon. J. Geophys. Res. 100 (B10), 20193–20210.

Personius, S.F., Kelsey, H.M., Grabau, P.C., 1993. Evidence for regional stream aggradation in the central Oregon Coast Range during the Pleistocene–Holocene transition. Quat. Res. 40, 297–308.

Reneau, S.L., Dietrich, W.E., 1991. Erosion rates in the southern Oregon Coast Range: evidence for an equilibrium between hillslope erosion and sediment yield. Earth Surf. Process. Landf. 16, 307–322.

Robison, E.G., Beschta, R.L., 1990. Identifying trees in riparian areas that can provide coarse woody debris to streams. For. Sci. 36 (3), 790–801.

Sidle, R.C., 1992. A theoretical model of the effects of timber harvesting on slope stability. Water Resour. Res. 28 (7), 1897–1910.

Sklar, L., Dietrich, W.E., 1998. River longitudinal profiles and bedrock incision models: stream power and the influence of sediment supply. In: Tinkler, K.J., Wohl, E.E. (Eds.), Rivers over Rock. Geophys. Monogr. Ser., vol. 107. American Geophysical Union, Washington, DC, pp. 237–260.

Sklar, L., Dietrich, W.E., 2001. Sediment and rock strength controls on river incision into bedrock. Geology 29 (12), 1087–1090.

Snyder, N.P., Whipple, K.X., Tucker, G.E., Merritts, D.J., 2000. Landscape response to tectonic forcing: digital elevation model analysis of stream profiles in the Mendocino triple junction region, northern California. Geol. Soc. Amer. Bull. 112 (8), 1250–1263.

Stock, J., Dietrich, W.E., 2003. Valley incision by debris flows: evidence of a topographic signature. Water Resour. Res. 39 (4), 1089. doi:10.1029/2001WR001057.

Stock, J.D., Montgomery, D.R., Collins, B.D., Dietrich, W.E., Sklar, L., 2005. Field measurements of incision rates following bedrock exposure: implications for process controls on the long-profiles of valleys cut by rivers and debris flows. Geol. Soc. Amer. Bull. 117 (11/12), 174–194. doi:10.1130/B25560.1.

Swanson, F.J., Lienkaemper, G.W., 1978. Physical consequences of large organic debris in Pacific Northwest streams. USDA For. Serv. Gen. Tech. Rep. PNW-69. 12 pp.

Swanson, F.J., 1977. Inventory of mass erosion in the Mapleton Ranger District, Siuslaw National Forest. Final Report, on file at Forestry Sciences Lab. Corvallis, OR, USA, 41 pp.

Van Sickle, J., Gregory, S.V., 1990. Modeling inputs of large woody debris to streams from falling trees. Can. J. For. Res. 20 (10), 1593–1601.

Whipple, K.X., Tucker, G.E., 1999. Dynamics of the stream-power river incision model: implications for height limits of mountain ranges, landscape response timescales, and research needs. J. Geophys. Res. 104 (B8), 17,661–17,674.

Whipple, K.X., Tucker, G.E., 2002. Implications of sediment-flux-dependent river incision models for landscape evolution. J. Geophys. Res. 107 (B2). doi:10.1029/2000JB000044.

Wolman, M.G., 1954. A method for sampling coarse river bed material. Trans.-Am. Geophys. Union 35, 951–956.

Worona, M., Whitlock, C., 1995. Late Quaternary vegetation and climate history near Little Lake, central Coast Range, Oregon. Geol. Soc. Amer. Bull. 107, 867–876.